

Polariton–dark exciton interactions in bistable semiconductor microcavitiesElena Rozas ^{1,*}, Evgeny Sedov ^{2,3,4}, Yannik Brune ¹, Sven Höfling ⁵, Alexey Kavokin ^{3,6,7} and Marc Aßmann ¹¹*Experimentelle Physik 2, Technische Universität Dortmund, D-44221 Dortmund, Germany*²*Russian Quantum Center, Skolkovo Innovation Center, Moscow 121205, Russia*³*Spin Optics Laboratory, St. Petersburg State University, 198504 St. Petersburg, Russia*⁴*Stoletov Vladimir State University, 600000 Vladimir, Russia*⁵*Technische Physik, Physikalisches Institut and Würzburg–Dresden Cluster of Excellence ct.qmat, Universität Würzburg, 97074 Würzburg, Germany*⁶*Key Laboratory for Quantum Materials of Zhejiang Province, School of Science, Westlake University, Hangzhou 310024, China*⁷*Institute of Natural Sciences, Westlake Institute for Advanced Study, Hangzhou 310024, China*

(Received 22 May 2023; revised 8 September 2023; accepted 26 September 2023; published 13 October 2023)

We take advantage of the polariton bistability in semiconductor microcavities to estimate the interaction strength between lower exciton-polariton and dark exciton states. We combine the quasiresonant excitation of polaritons and the nominally forbidden two-photon excitation (TPE) of dark excitons in a GaAs microcavity. To this end, we use an ultranarrow linewidth cw laser for the TPE process that allows us to determine the energy of dark excitons with high spectral resolution. Our results evidence a sharp drop in the polariton transmission intensity and width of the hysteresis cycle when the TPE process is resonant with the dark exciton energy, highly compromising the bistability of the polariton condensate. This behavior demonstrates the existence of a small symmetry breaking such as that produced by an effective in-plane magnetic field, allowing us to directly excite the dark reservoir. We numerically reproduce the collapse of the hysteresis cycle with the increasing dark exciton population, treating the evolution of a polariton condensate in a one-mode approximation, coupled to the exciton reservoir via polariton-exciton scattering processes.

DOI: [10.1103/PhysRevB.108.165411](https://doi.org/10.1103/PhysRevB.108.165411)**I. INTRODUCTION**

Optically inactive dark excitons have attracted much attention due to their promising prospects for information processing [1–4] and the creation of long-lasting potentials due to their stable nonradiative nature. For the same reason, applying optical spectroscopy methods for probing them is challenging as one cannot optically excite them and they do not emit light. Thus, dark excitons are not directly accessible by the means of spectroscopy. To reveal and exploit their properties, one has to resort to alternative approaches. For spin-forbidden dark excitons, on which we focus in this manuscript, the use of external in-plane magnetic fields has been examined to induce a mixing of bright and dark states to make spectroscopy experiments possible [5,6]. This technique enabling redistribution of the weight coefficients between bright and dark states by changing the direction and magnitude of the magnetic field has been studied both experimentally and theoretically in quantum wells (QWs) and quantum dots [7–11]. Nevertheless, strong magnetic fields are not routinely available in every laboratory. In addition, strong mixing of dark and bright excitons leads to a significant change in their properties. The presence of a weak symmetry breaking is another option for dark excitons to be accessible via two-photon absorption processes and to allow new transitions. Optical transitions are usually dipole-allowed in

one-photon processes and forbidden in two-photon processes, which makes two-photon excitation (TPE) a very selective tool for studying them.

Typically one needs ultrashort pulsed lasers with high peak powers to achieve reasonable TPE efficiencies. This results in a limitation of the achievable spectral resolution. Even worse, at high peak powers second-harmonic generation (SHG) may occur, which may excite bright excitons spectrally close to the dark ones, as in the case of confined systems such as QWs. This is especially common for GaAs-based QWs [12–14]. However, when they are embedded inside a high-quality microcavity, polaritons form the bright states and are shifted away from the dark states by the Rabi energy. This increases the bright-dark splitting from a few microelectronvolts for bare quantum wells to about 10 meV for a polariton system, which eliminates the possibility of direct excitation of bright states via SHG.

Exciton polaritons inherit unique properties from both of their components. The excitonic fraction confers on polaritons the ability to interact with each other as well as with excitons and charge carriers [15]. The photonic fraction ensures high mobility of polaritons due to the low effective mass and provides direct access to the properties of the system through their photoluminescence. As a result, polaritons have been extensively studied both experimentally and theoretically for their potential applications in quantum optics encouraged by their key role in a wide number of fundamental nonlinear effects including polariton lasing [16–19], superfluidity [20–24], polariton-mediated superconductivity [25,26],

*elena.rozas@tu-dortmund.de

persistent polariton currents [27,28], quantized vortices [29–35], and Bose-Einstein condensation [36–44]. Polariton condensates, while fundamentally driven fluids arising from the driven-dissipative nature of polaritons, are referred to as condensates in this work for simplicity, despite their inherently nonequilibrium state. The origin of such strong nonlinearities lies in the spin-anisotropic polariton-polariton interaction, which is repulsive for like-oriented spins, and manifests itself as a blueshift of the polariton energy [45].

Despite the optical inactivity of dark excitons, they may contribute to a wide range of peculiar effects observed in polariton condensates via their interactions with polaritons. In particular, oscillations in the polariton population resembling quantum beats between bright and dark excitons have been observed in the nonlinear regime, which has been explained as a consequence of electron exchange [46]. To obtain experimental access to the interactions between dark excitons and polaritons, we take advantage of the optical bistability exhibited by polaritons when excited in transmission geometry. Bistability in macroscopic coherent polariton systems refers to a phenomenon where the system exhibits two distinct stable states under the same external conditions. This means that for a certain range of excitation power or other relevant parameters, e.g., detuning of the excitation laser energy from the polariton energy, the polariton system can exist in either a low-intensity state or a high-intensity state, with a sharp transition between the two states. Such bistable behavior is a consequence of the system's nonlinearity, which affects the energy of the polariton state. It can occur when the polariton mode approaches the resonance of the excitation laser, triggering the appearance of a hysteresis cycle between two well-defined states [47–50].

The use of polariton bistability has already been demonstrated as a sensitive probe for tracking the presence and dynamics of dark carriers in semiconductors. A recent experimental study by Schmidt *et al.* found long-lived dark excitons (>20 ns) nonresonantly injected into InGaAs quantum wells by monitoring their interaction with lower branch polaritons [51]. The existence of such bistable behavior evidences the presence of an effective internal memory, revealing its prospects for designing memory elements and optical transistors.

In this work, we propose an approach to quantify the interaction between polaritons and dark excitons based on the analysis of the polariton bistability. To do so, we combine the quasis resonant excitation of lower exciton-polaritons and the TPE of dark excitons. For any system, TPE processes not only require that two photons are absorbed simultaneously, but that those photons arrive at the sample at exactly the same time. To initiate this process, a higher laser power compared to that used for one-photon excitation is required, which is essential for increasing the photon density and, consecutively, the probability of absorption. Sources of ultrashort laser pulses have been widely used for this purpose since they provide a huge number of photons per pulse, i.e., the shorter the pulse, the higher the peak photon flux. However, pulsed lasers also show a broad energy spectrum which limits the obtainable spectral resolution. To overcome this conundrum, we use the high sensitivity of the polariton bistability for detecting weakly populated dark exciton states. This allows

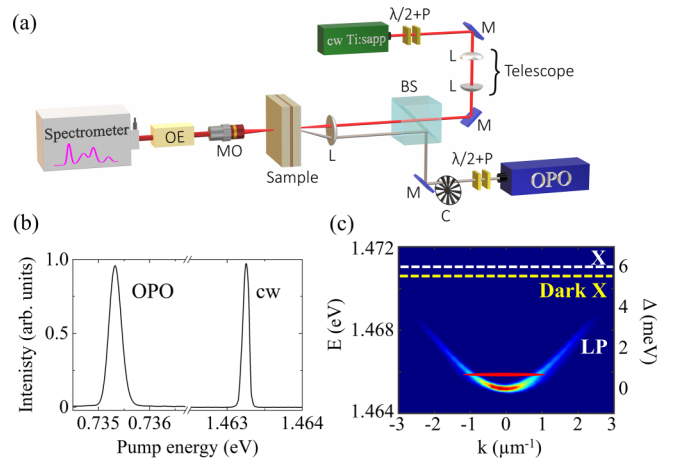


FIG. 1. (a) Sketch of the experimental setup consisting of a continuous wave laser (cw), optical parametric oscillator (OPO), half-wave plates ($\lambda/2$), linear polarizers (P), mirrors (M), plano-convex lenses (L), optical chopper system (C), beam splitter (BS), microscope objective (MO), and several optical elements (OEs) for the realization of real and Fourier spectroscopy. (b) Normalized laser spectrum of the OPO and cw sources. (c) Angle-resolved photoluminescence of the sample under nonresonant optical pumping. The dispersion of lower polaritons (LPs) is clearly seen [52]. Dashed lines indicate energy levels of bright (X) and dark (Dark X) excitons. The energy of the cw laser is indicated by a red line.

us to examine dark excitons using an ultranarrow linewidth cw laser with high spectral resolution. The possibility of fine-tuning the laser frequency enables us to carefully scan the eigenenergy spectrum of the sample and to identify the dark exciton energy. One should note that the possibility of direct excitation of spin-forbidden carriers even in the absence of an external magnetic field indicates a weak symmetry breaking inherent in our system. As a consequence, we observe a significant shift in the hysteresis thresholds introduced by the dark carriers. We reproduce the effect numerically by solving the generalized Gross-Pitaevskii equation, taking into account the condensate energy blueshift introduced by the dark exciton reservoir. The simulation allows us to estimate the strength of the polariton-exciton interaction responsible for the shift of the thresholds.

II. SAMPLE AND SETUP

The sample used in this work is a planar GaAs λ cavity grown by molecular beam epitaxy. Six $\text{In}_{0.1}\text{Ga}_{0.9}\text{As}$ quantum wells are placed at the antinode positions of the electric field confined by two distributed Bragg reflectors (DBRs). The top (bottom) DBR structures consist of 26 (30) pairs of alternating layers of GaAs and AlAs. The microcavity provides a Rabi splitting of polariton eigenmodes of $V_R = 6$ meV. A wedge introduced in the cavity allows modifying the cavity-exciton detuning during the experiments.

A schematic of the experimental setup is displayed in Fig. 1(a). The sample was mounted in a helium-flow cryostat at a fixed temperature of 10 K. To create the polariton population, the cavity was excited quasis resonantly under normal incidence with a cw Ti:sapphire mode-locked laser detuned

by 700 μeV above the LP ground-energy state. Additionally, an Aculight Argos MgO:PPLN optical parametric oscillator (OPO) with a tunable output wavelength was used for the TPE of dark excitons. In the experiment, the OPO beam was focused onto the sample under an incidence angle of 17° . Its energy was initially tuned to half the energy of the LP state and gradually shifted towards the exciton level, i.e., $2E_{\text{OPO}} = E_{\text{LP}} + \Delta$, where Δ is the energy shift with respect to the initial lower polariton energy. To avoid possible heating effects due to the high excitation power used, the OPO beam was modulated by an optical chopper with a 10% duty cycle. An example of the energy profiles of both laser beams is shown in Fig. 1(b). The measured spectral linewidths are $<100 \mu\text{eV}$ and $<300 \mu\text{eV}$ for the cw and the OPO, respectively. The use of such narrow linewidths is crucial when scanning and determining the energy distribution of dark excitons. Both beams were vertically polarized, parallel to the TM mode of the cavity, and focused onto the sample with a spot size of 28 μm . An optical telescope was added to the setup to ensure the full overlap between both excitation spots. The light transmitted through the sample was collected at normal incidence using a $10\times$ microscope objective with a numerical aperture of 0.26 and guided to a Si photodiode.

For the correct assessment of the above conditions, the far-field emission from the sample was first collected under nonresonant pumping conditions by tuning the cw source to the first minimum of the DBR stop-band at 1.686 eV. Figure 1(c) shows the obtained quasimomentum distribution of lower polaritons with the bottom of the dispersion curve at 1.465 eV. The bare QW exciton level (X) is indicated with a white dashed line at $E_x = 1.471$ eV. The tentative dark exciton level is highlighted with a yellow dashed line at lower energy, which is expected to have a large energy separation from X at $k = 0$. To induce optical bistability in the sample, it is imperative to set the cw laser under quasiresonant conditions. However, a bistable behavior is obtained only when the detuning between the cw laser frequency and the LP resonance exceeds a certain threshold. This threshold is defined by the inequality $\delta_{\text{th}} > \sqrt{3}\gamma_p$, where γ_p is the polariton linewidth [48]. We extract from the polariton dispersion shown in Fig. 1(c) a linewidth of $\gamma_p \approx 190 \mu\text{eV}$, setting the threshold at $\delta_{\text{th}} \approx 330 \mu\text{eV}$. Note that variations in the polariton linewidth might emerge with changes in the cavity-exciton detuning, resulting in a modification of the δ_{th} value with the sample position. For this reason, we positioned the cw laser at $2\delta_{\text{th}} \approx 700 \mu\text{eV}$ above the LP ground-state energy [red solid line in Fig. 1(c)], which ensures a considerable distance from the fluctuating threshold. Following this configuration, the OPO laser was then added to the setup. For a better understanding, in the following we will refer to the OPO energy in terms of the energy shift Δ with respect to the unshifted lower polariton energy.

III. DARK EXCITON RESERVOIR

Different mechanisms may contribute to the formation of a dark exciton reservoir, so one should consider which ones are expected to take place in our experiment. First, excitons propagating with large in-plane momenta in the QW plane

are optically dark. Since their momenta are beyond the linear photon dispersion (the light cone), they are unable to couple to photons directly. Consequently, the presence of these excitons has been poorly studied because of the inaccessibility of their properties by conventional optical methods. Nonetheless, they have been predicted in low-dimensional semiconductor systems such as QWs and transition-metal dichalcogenide monolayers [53]. The most prominent pathway of their assembly is the spontaneous formation of excitons from free carriers. They are therefore highly relevant for the nonresonant excitation of polaritons via excitation above the band gap, but they are not expected to be relevant for the resonant excitation used in our experiment. Thus, dark excitons within the light cone, where the simultaneous conservation of energy and momentum in optical transitions are in principle possible, but orbital or spin quantum number selection rules render one-photon transitions forbidden, are more appropriate candidates in our study. The relevant states that are dark due to orbital quantum number selection rules are given by excited exciton states carrying nonzero orbital angular momentum, such as p -, d -, or f -excitons. In particular, p -exciton states may be excited resonantly via two-photon absorption [54–56]. However, the $2p$ -state as the lowest energy p -state exciton is about 10 meV above the $1s$ -exciton state [57], which is above the range of energies we investigate in this study. Therefore, we will also not be able to observe the direct excitation of p -excitons in our experiment.

Another type of dark exciton state is given by excitons with spin-forbidden transitions. Unlike bright excitons, which arise as a result of the interaction of electrons and holes with antiparallel spins, this type of dark exciton is formed by electrons and holes with parallel spins and acquires the pseudospin $J = 2$ and a spin projection M_J . Due to the optical selection rules, they are also optically inactive. As the operators representing electric dipole transitions do not operate on spin space, this is still true in two-photon absorption based on electric dipole transitions. However, two possible excitation pathways remain. Transitions to dark exciton states with $J = 2$ and $M_J = \pm 1$ are allowed due to magnetic dipole two-photon absorption [58], but very weak. Also, for dark excitons with $J = 2$ and $M_J = \pm 2$, a symmetry breaking may result in mixing between the dark $J = 2$ and the bright $J = 1$ states, enabling the optical excitation of spin-forbidden states and their subsequent interaction with polaritons. This symmetry breaking is commonly introduced by an external magnetic field or by an effective magnetic field, e.g., due to spin-orbit coupling. As we do not apply external magnetic fields, we expect the mixing between dark and bright states also to be weak. In the following, we will show that although these transitions to the spin-forbidden exciton states are only weakly allowed, they have a significant effect on the bistability we observe in the transmission through a polariton microcavity.

It is also worth mentioning that structures with multiple QWs of quantity N exhibit a combination of bright polariton eigenmodes, accompanied by $N - 1$ dark exciton eigenmodes. The presence of any disorder within each particular QW may result in the “brightening” of these dark modes, partially mixing them with bright modes. This mixing typically leads to the broadening of their linewidth [59]. This

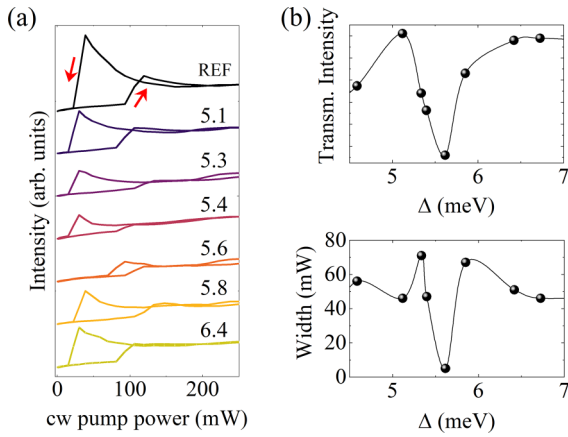


FIG. 2. (a) Transmitted intensity as a function of the cw pump power for different values of Δ (in meV). The hysteresis cycle in the absence of OPO is labeled as REF. For the rest of the profiles, a constant OPO pump power of 1.6 W was used. Red arrows indicate the direction of the tuned power. (b) Transmitted intensity of the ON-state at 70 mW (top) and width of the hysteresis cycle (bottom). Both magnitudes exhibit a dramatic drop at the same value, $\Delta = 5.6$ meV. The plots correspond to a section of the sample with $\delta_{C-X} = -4.5$ meV.

enables us to rule out these modes as candidates for the role of long-lived dark excitons, which are the focus of our study.

To identify the influence of the dark exciton reservoir, in Fig. 2(a) we show the transmitted intensity of the polariton emission at a detuning of $\delta_{C-X} = -4.5$ meV. When only the resonant cw pump is applied (REF), near 95 mW the emission indicates a sudden nonlinear increase of the polariton population with increasing pump power. During this transition, the ground mode experiences an energy blueshift as a consequence of the polariton-polariton interaction, shifting the cavity mode closer into resonance with the laser, which in turn increases the number of created polaritons, and, eventually, the system switches into the ON-state. When the incident pump power is reduced, the cavity-laser resonance remains stable, keeping the system in the ON-state until the power drops below a critical power of 39 mW, which switches the system back to the OFF-state. The region where both states are stable is known as the bistable region. It is bounded by two power thresholds that define the switching to the ON- and OFF-states, which we refer to as the upper and the lower thresholds. Weak changes in the hysteresis loop are observed when the OPO excitation is added to the setup with a pump power of 1.6 W, affecting the transmitted intensity and the thresholds of the bistable region; see Fig. 2(a). However, the bistability region reduces considerably when Δ is tuned close to 5.6 meV. This effect is best illustrated in Fig. 2(b), which shows the change of the transmitted intensity in the ON-state and the loop width with Δ . The considerable drop in both magnitudes experienced at the same energy indicates the interaction of polaritons with additional carriers emerging in the system. This interaction contributes to the blueshift of the polariton energy, and a lower density of polaritons is required to shift the system into the ON-state. It should be emphasized that the smooth shape of both curves in the vicinity of the

minimum can give us an idea about the spectral linewidth of these carriers.

We attribute this effect to the formation of a spin-forbidden dark exciton reservoir when the OPO is set to $\Delta = 5.6$ meV. Let us stress again that in microcavity structures at $k = 0$, the energy splitting between bright and dark exciton states is given by the Rabi splitting and is therefore much larger compared to bare quantum wells, so there are no bright states in the vicinity of the two-photon OPO energy. Hence, we can estimate the energy of dark excitons as $E_D = 1.4708 \pm 0.0003$ eV, which is consistent with the already observed energy splitting between bright and spin-forbidden 1s exciton dark states in bare QWs [14,60]. The error has been determined by the wavelength resolution of the OPO and the data extracted from the polariton system. Note that heating effects can be safely ruled out as a possible source of the observed effect as heating would be equally noticeable for all OPO energies. Furthermore, we repeated the above procedure for several cavity-exciton detunings, consistently achieving the same energy for dark excitons in all cases, as one would expect due to the flat dispersion band of excitons [61].

Although the direct optical excitation of these spin-forbidden 1s exciton states is at most very weakly allowed in the TPE regime, we also find a small but characteristic nonlinear increase in the total absorption of the OPO light by the sample, when the OPO is tuned exactly to $\Delta = 5.6$ meV (see the Supplemental Material [61]). Accordingly, we have shown that the polariton bistability is indeed a highly sensitive tool for detecting a small population of dark exciton states.

IV. POLARITON-DARK EXCITON INTERACTION

The strength of the interaction between polaritons and dark excitons is considerably dependent on their population densities, and it can be adjusted by tuning the incident cw and OPO pump power. To evaluate the interaction strength via the formation of the polariton condensate, we investigate the dependence of the transmitted intensity with different OPO powers. To better illustrate this process, we shift our attention to a sample region with $\delta_{C-X} = 0.4$ meV. By adopting a positive δ_{C-X} , polaritons are less susceptible to disorder and localization effects. Consequently, we mitigate the influence of spatial disorder compared to negative detunings. This allows us to carefully observe small variations in the polariton occupancy and the condensation threshold caused by the presence of the dark reservoir. For this experiment, the OPO energy was set to the resonant dark exciton energy level, and its power was tuned in the range [0, 1.9] W. Heating effects arising from the presence of such an intense OPO beam were experimentally ruled out (i) by using an optical chopper, (ii) by accurately monitoring the lattice temperature, and (iii) by the fact that heating would have affected the experimental data in the same way for all OPO pump energies, which contradicts the results of our previous observations. It is also important to emphasize that chopping the OPO beam is not detrimental to the bistability as the cw laser is still switched on constantly. Figure 3(a) depicts the polariton occupancy with increasing cw pump power for different OPO powers. When polaritons interact with the dark reservoir created by the OPO, it causes the polariton system to switch to the ON-state at

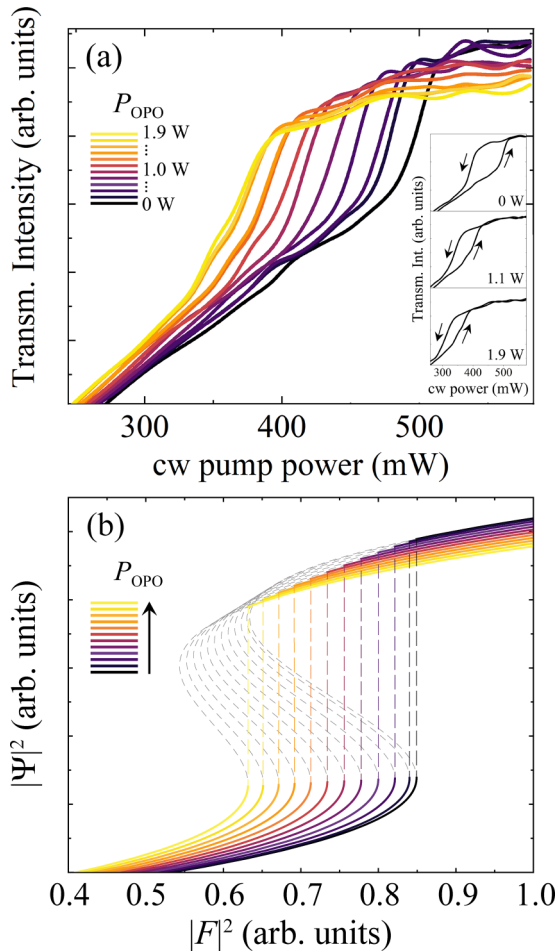


FIG. 3. Polariton occupancy vs increasing cw pump power for different OPO pump powers. (a) Results of experimental observations at $E_{\text{OPO}} = 1/2E_{\text{D}}$ and an OPO pump power ranging between 0 and 1.9 W. The profiles are detected in a region of the sample with $\delta_{\text{C-X}} = 0.4$ meV. The inset shows the complete measured hysteresis loops with increasing and decreasing cw pump power for $P_{\text{OPO}} = 0, 1.1,$ and 1.9 W. (b) Results of numerical simulations obtained by solving Eq. (2). P_{OPO} increases for curves from black to yellow. For the simulations, we take $|X|^2 = 0.54$, $\hbar\omega_{\text{p}} = 0.675$ meV, and $\hbar\gamma = 0.283$ meV.

lower cw powers. Specifically, the perturbation caused by the dark reservoir is manifested as a shift of the upper threshold from about 500 to 350 mW when the OPO power changes from 0 to 1.9 W. Consequently, the bistable region undergoes a significant reduction in its width. In the inset of Fig. 3(a), the complete hysteresis loop is illustrated for certain P_{OPO} values, revealing a gradually narrower region. It is worth noting that this reduction is also attributed to a further displacement of the lower threshold. Interestingly, the occupation of the ON-state displays a slight yet constant decrease as P_{OPO} increases. In addition, we observed how larger dark exciton densities lead to a gentler nonlinear transition between the OFF- and ON-states, thereby reducing the sharper slope initially observed.

In Fig. 3(b), we support our experimental observations with a numerical simulation of the coevolution of the polariton condensate under the cw pump and the dark reservoir excited by the OPO pump. Following [51,62], we solve a one-mode

generalized Gross-Pitaevskii equation for the polariton condensate wave function Ψ , coupled to the rate equation for the occupation number N_{D} of the dark reservoir:

$$id_t\Psi = [-\omega_{\text{p}} + \alpha_{\text{PP}}|\Psi|^2 + \alpha_{\text{PX}}N_{\text{D}}]\Psi - i\gamma\Psi + f, \quad (1a)$$

$$d_tN_{\text{D}} = W_{\text{OPO}} + \beta|f|^2 - (\gamma_{\text{D}} + AN_{\text{D}})N_{\text{D}}. \quad (1b)$$

We use the dark exciton interaction constant α_{XX} as a fitting parameter. In principle, we also need to consider the interaction constants $\alpha_{\text{XX,BD}}$ between bright and dark excitons and $\alpha_{\text{XX,BB}}$ between two bright excitons separately. However, all of them are expected to be at least similar in magnitude [63], so we minimize the number of fitting parameters by defining $\alpha_{\text{PX}} = |X|^2\alpha_{\text{XX}}/2N_{\text{QW}}$ and $\alpha_{\text{PP}} = |X|^2\alpha_{\text{PX}}$ as the polariton-exciton and polariton-polariton interaction constants, respectively. $|X|^2$ determines the exciton fraction in the polariton state, and N_{QW} is the number of QWs in the cavity [64]. γ and γ_{D} are the polariton and dark reservoir exciton decay rates, respectively. A characterizes the nonlinear losses in the reservoir that may result from, e.g., Auger processes.

The coherent polariton state is excited by the cw resonant optical pump $f = CF$ of the amplitude F . The pumping efficiency is determined by the fraction of the photonic component C in the polariton state, $|C|^2 = 1 - |X|^2$ [52]. ω_{p} is the frequency of the resonant pump with respect to the bottom of the polariton dispersion. The term $\beta|f|^2$ characterizes partial filling of the reservoir under the resonant pumping, and β is the reservoir response constant [51]. W_{OPO} is the two-photon excitation rate for the reservoir, which is related to the OPO pump power as follows [65,66]: $W_{\text{OPO}} = \eta P_{\text{OPO}}^2/2E_{\text{OPO}}$, where η is the absorption coefficient and a fitting parameter of the model.

For the driven polariton mode, Eqs. (1) reduce to

$$|CF|^2|\Psi|^{-2} = (\omega_{\text{p}} - \alpha_{\text{PP}}|\Psi|^2 - \alpha_{\text{PX}}N_{\text{D}})^2 + \gamma^2 \quad (2)$$

with $N_{\text{D}} = (W_{\text{OPO}} + \beta|CF|^2)/(\gamma_{\text{D}} + AN_{\text{D}})$. In Fig. 3(b) the hysteresis loops on the $(|F|^2, |\Psi|^2)$ plane are shown for different pump powers, P_{OPO} , obtained by solving Eq. (2). The simulations reproduce both the decrease in the upper threshold and the reduction of the loop width with increasing OPO powers. Notably, the experimentally observed decrease in the occupancy of the ON-state with larger dark exciton densities is also reproduced by our numerical model.

We now focus on the thresholds of the bistable region. The thresholds found from the condition $d|F|^2/d|\Psi|^2 = 0$ are given as follows:

$$|F|_{\text{th}}^2 = \frac{2}{27|C|^2\alpha_{\text{PP}}} [\bar{\omega}_{\text{p}}(\bar{\omega}_{\text{p}}^2 + 9\gamma^2) \pm (\bar{\omega}_{\text{p}}^2 - 3\gamma^2)\sqrt{\bar{\omega}_{\text{p}}^2 - 3\gamma^2}], \quad (3)$$

where $\bar{\omega}_{\text{p}} = \omega_{\text{p}} - \alpha_{\text{PX}}N_{\text{D}}$ is the effective pump frequency offset, which takes into account the reservoir-induced energy blueshift. In our study, for completeness, we consider two different cavity detunings, 0.4 and 4.6 meV, which result in different exciton fractions of the polaritons. The displacement of the upper and lower thresholds with P_{OPO} is shown in Fig. 4. The experimental values (black circles and green diamonds) were taken as midpoints of the transitions between the OFF- and ON-states. Shaded areas indicate the full widths

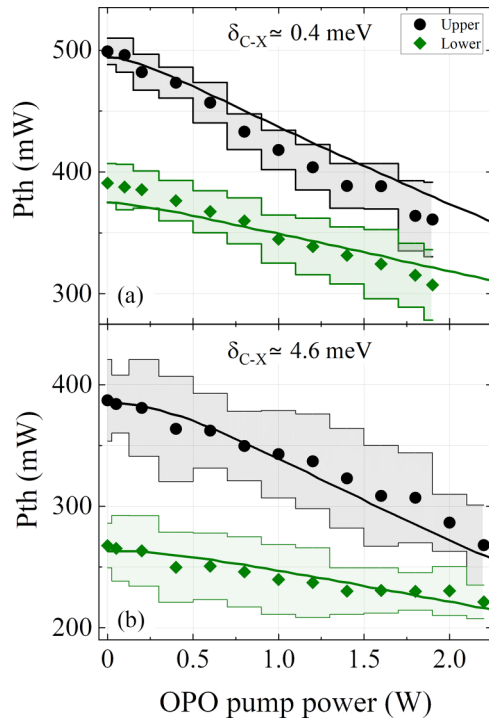


FIG. 4. Upper (black) and lower (green) power thresholds defining the hysteresis cycle as a function of the OPO pump power. Parts (a) and (b) correspond to δ_{C-X} of 0.4 and 4.6 meV, respectively. Solid lines show the results of the numerical simulations. For the latter, we take (a) $|X|^2 = 0.54$, $\hbar\omega_p = 0.675$ meV, $\hbar\gamma = 0.283$ meV and (b) $|X|^2 = 0.8$, $\hbar\omega_p = 0.675$ meV, $\hbar\gamma = 0.24$ meV.

of the transitions. A significant difference of 100 mW in the threshold values for the two detunings can be attributed to the excitonic content of the polaritons. In general, the turning points of the bistability loop are determined by the detuning between the excitation beam energy and the energy of the resonant coherent polariton state [49,67]. The latter is influenced by the exciton reservoir, which induces the energy blueshift. The magnitude of the blueshift is determined by the population of the reservoir N_D and the repulsive interaction constant between the reservoir and the polariton state α_{PX} , which is subject to modification with changes in the exciton fraction. Consequently, for the same reservoir population, a larger blueshift, and hence a smaller detuning from the excitation energy $\bar{\omega}_p$, are reached for more excitonlike lower branch polaritons, corresponding to a larger-in-magnitude positive exciton-photon detuning δ_{C-X} . As a result, according to (3), the magnitude of the bistability threshold decreases with an increasing exciton-photon detuning δ_{C-X} , which is confirmed in Fig. 4.

The simulated dependencies of the thresholds of the hysteresis loop on the OPO pump power are shown in Fig. 4 with solid lines, supplementing the experimental observation results. The dark reservoir decay rate was taken as $\gamma_D = 1/22$ ns⁻¹ matching the previous experimental estimations of the parameter in the same sample [51]. The best fit

was achieved for the fitting parameters $A = 1.5 \times 10^{-6}$ ps⁻¹ and $\eta = 4 \times 10^{-4}$, which gives the estimation of the exciton-exciton interaction constant as $\alpha_{XX} = 61$ $\mu\text{eV } \mu\text{m}^2$. Our estimations are further supported by the fact that the polariton-polariton interaction constant then takes the value of $\alpha_{PP} = 1.8$ $\mu\text{eV } \mu\text{m}^2$, which is in good agreement with previous estimations in InGaAs QWs [68–70], especially when considering that the interaction constant for condensed polaritons is generally lower than for uncondensed ones [71]. Our simulations show that despite the dark nature of the reservoir, its interaction with bright polariton states takes place in the bistable microcavity system with an interaction constant estimated as $\alpha_{PX} \simeq 3$ $\mu\text{eV } \mu\text{m}^2$.

V. CONCLUSIONS

In summary, we have developed an approach to accessing the properties of spin-forbidden dark excitons in QWs embedded in optical microcavities. The approach is based on spectroscopic measurements utilizing an ultranarrow linewidth cw laser for the TPE of spin-forbidden dark excitons in the regime of polariton bistability. In the experiment, we studied the peculiar dependence of the photoluminescence of the polariton state on the cw pump power under its interaction with dark excitons. The accumulation of long-living optically inactive excitons localized under the pump spot causes a shift of the condensate up to higher energies as well as a reduction of the condensation threshold power. The experimental observations have been reproduced numerically, including the shift of the bistability thresholds and the reduction in width of the bistability loop. Based on a comparison of the results of experimental observations and numerical simulations, we were able to estimate the interaction constant of polaritons and dark excitons with each other and among themselves. Due to their long lifetimes and robustness, dark excitons are excellent candidates for creating functional potentials in polariton condensates. Knowing the exciton-polariton interaction constant is therefore a decisive factor in the engineering of optical polariton devices and enables their deterministic control.

ACKNOWLEDGMENTS

This work was supported by the Deutsche Forschungsgemeinschaft through the International Collaborative Research Centre TRR 160, Grant No. 249492093 (project B7). E.S. acknowledges state assignment in the field of scientific activity of the RF Ministry of Science and Higher Education (theme FZUN-2020-0013, state assignment of VISU). Numerical calculations of the hysteresis thresholds were supported by the Russian Science Foundation (Grant No. 19-72-20039). E.S. and A.K. acknowledge Saint-Petersburg State University (Grant No. 94030557). A.K. acknowledges the support of the Russian Foundation for Basic Research (RFBR), Project No. 19-52-12032, Westlake University, Project No. 041020100118 and Program 2018R01002 funded by the Leading Innovative and Entrepreneur Team Introduction Program of Zhejiang Province of China.

- [1] T. Heindel, A. Thoma, I. Schwartz, E. R. Schmidgall, L. Gantz, D. Cogan, M. Strauß, P. Schnauber, M. Gschrey, J.-H. Schulze, A. Strittmatter, S. Rodt, D. Gershoni, and S. Reitzenstein, Accessing the dark exciton spin in deterministic quantum-dot microlenses, *APL Photon.* **2**, 121303 (2017).
- [2] I. Schwartz, E. R. Schmidgall, L. Gantz, D. Cogan, E. Bordo, Y. Don, M. Zielinski, and D. Gershoni, Deterministic writing and control of the dark exciton spin using single short optical pulses, *Phys. Rev. X* **5**, 011009 (2015).
- [3] E. Poem, Y. Kodriano, C. Tradonsky, N. H. Lindner, B. D. Gerardot, P. M. Petroff, and D. Gershoni, Accessing the dark exciton with light, *Nat. Phys.* **6**, 993 (2010).
- [4] J. McFarlane, P. A. Dalgarno, B. D. Gerardot, R. H. Hadfield, R. J. Warburton, K. Karrai, A. Badolato, and P. M. Petroff, Gigahertz bandwidth electrical control over a dark exciton-based memory bit in a single quantum dot, *Appl. Phys. Lett.* **94**, 093113 (2009).
- [5] X.-X. Zhang, T. Cao, Z. Lu, Y.-C. Lin, F. Zhang, Y. Wang, Z. Li, J. C. Hone, J. A. Robinson, D. Smirnov, S. G. Louie, and T. F. Heinz, Magnetic brightening and control of dark excitons in monolayer WSe_2 , *Nat. Nanotechnol.* **12**, 883 (2017).
- [6] Z. Lu, D. Rhodes, Z. Li, D. V. Tuan, Y. Jiang, J. Ludwig, Z. Jiang, Z. Lian, S.-F. Shi, J. Hone, H. Dery, and D. Smirnov, Magnetic field mixing and splitting of bright and dark excitons in monolayer MoSe_2 , *2D Mater.* **7**, 015017 (2019).
- [7] T. S. Shamirzaev, J. Rautert, D. R. Yakovlev, J. Debus, A. Y. Gornov, M. M. Glazov, E. L. Ivchenko, and M. Bayer, Spin dynamics and magnetic field induced polarization of excitons in ultrathin GaAs/AlAs quantum wells with indirect band gap and type-II band alignment, *Phys. Rev. B* **96**, 035302 (2017).
- [8] T. S. Shamirzaev, J. Rautert, D. R. Yakovlev, and M. Bayer, Exciton recombination and spin relaxation in strong magnetic fields in ultrathin (In,Al)As/AlAs quantum wells with indirect band gap and type-I band alignment, *Phys. Rev. B* **104**, 045305 (2021).
- [9] D. Caputo, E. S. Sedov, D. Ballarini, M. M. Glazov, A. V. Kavokin, and D. Sanvitto, Magnetic control of polariton spin transport, *Commun. Phys.* **2**, 165 (2019).
- [10] E. S. Sedov, I. E. Sedova, S. M. Arakelian, and A. V. Kavokin, Magnetic control over the zitterbewegung of exciton-polaritons, *New J. Phys.* **22**, 083059 (2020).
- [11] R. M. Stevenson, R. J. Young, P. See, D. G. Gevaux, K. Cooper, P. Atkinson, I. Farrer, D. A. Ritchie, and A. J. Shields, Magnetic-field-induced reduction of the exciton polarization splitting in InAs quantum dots, *Phys. Rev. B* **73**, 033306 (2006).
- [12] M. Z. Maialle, E. A. de Andrada e Silva, and L. J. Sham, Exciton spin dynamics in quantum wells, *Phys. Rev. B* **47**, 15776 (1993).
- [13] M. Vladimirova, S. Cronenberger, D. Scalbert, K. V. Kavokin, A. Miard, A. Lemaître, J. Bloch, D. Solnyshkov, G. Malpuech, and A. V. Kavokin, Polariton-polariton interaction constants in microcavities, *Phys. Rev. B* **82**, 075301 (2010).
- [14] A. V. Trifonov, E. S. Khramtsov, K. V. Kavokin, I. V. Ignatiev, A. V. Kavokin, Y. P. Efimov, S. A. Eliseev, P. Y. Shapochkin, and M. Bayer, Nanosecond spin coherence time of nonradiative excitons in GaAs/AlGaAs quantum wells, *Phys. Rev. Lett.* **122**, 147401 (2019).
- [15] J. Schmutzler, T. Kazimierczuk, O. Bayraktar, M. Aßmann, M. Bayer, S. Brodbeck, M. Kamp, C. Schneider, and S. Höfling, Influence of interactions with noncondensed particles on the coherence of a one-dimensional polariton condensate, *Phys. Rev. B* **89**, 115119 (2014).
- [16] D. Bajoni, Polariton lasers. Hybrid light–matter lasers without inversion, *J. Phys. D* **45**, 313001 (2012).
- [17] E. Kammann, H. Ohadi, M. Maragkou, A. V. Kavokin, and P. G. Lagoudakis, Crossover from photon to exciton-polariton lasing, *New J. Phys.* **14**, 105003 (2012).
- [18] C. Schneider, A. Rahimi-Iman, N. Y. Kim, J. Fischer, I. G. Savenko, M. Amthor, M. Lerner, A. Wolf, L. Worschech, V. D. Kulakovskii, I. A. Shelykh, M. Kamp, S. Reitzenstein, A. Forchel, Y. Yamamoto, and S. Höfling, An electrically pumped polariton laser, *Nature* **497**, 348 (2013).
- [19] S. Kim, B. Zhang, Z. Wang, J. Fischer, S. Brodbeck, M. Kamp, C. Schneider, S. Höfling, and H. Deng, Coherent polariton laser, *Phys. Rev. X* **6**, 011026 (2016).
- [20] G. Malpuech, D. D. Solnyshkov, H. Ouerdane, M. M. Glazov, and I. Shelykh, Bose glass and superfluid phases of cavity polaritons, *Phys. Rev. Lett.* **98**, 206402 (2007).
- [21] S. Utsunomiya, L. Tian, G. Roumpos, C. W. Lai, N. Kumada, T. Fujisawa, M. Kuwata-Gonokami, A. Löffler, S. Höfling, A. Forchel, and Y. Yamamoto, Observation of Bogoliubov excitations in exciton-polariton condensates, *Nat. Phys.* **4**, 700 (2008).
- [22] A. Amo, J. Lefrère, S. Pigeon, C. Adrados, C. Ciuti, I. Carusotto, R. Houdré, E. Giacobino, and A. Bramati, Superfluidity of polaritons in semiconductor microcavities, *Nat. Phys.* **5**, 805 (2009).
- [23] A. Amo, D. Sanvitto, F. P. Laussy, D. Ballarini, E. d. Valle, M. D. Martin, A. Lemaître, J. Bloch, D. N. Krizhanovskii, M. S. Skolnick, C. Tejedor, and L. Viña, Collective fluid dynamics of a polariton condensate in a semiconductor microcavity, *Nature* **457**, 291 (2009).
- [24] I. Amelio and I. Carusotto, Perspectives in superfluidity in resonantly driven polariton fluids, *Phys. Rev. B* **101**, 064505 (2020).
- [25] F. P. Laussy, A. V. Kavokin, and I. A. Shelykh, Exciton-Polariton mediated superconductivity, *Phys. Rev. Lett.* **104**, 106402 (2010).
- [26] E. Sedov, I. Sedova, S. Arakelian, G. Eramo, and A. Kavokin, Hybrid optical fiber for light-induced superconductivity, *Sci. Rep.* **10**, 8131 (2020).
- [27] E. S. Sedov, V. A. Lukoshkin, V. K. Kalevich, P. G. Savvidis, and A. V. Kavokin, Circular polariton currents with integer and fractional orbital angular momenta, *Phys. Rev. Res.* **3**, 013072 (2021).
- [28] E. Sedov, V. Lukoshkin, V. Kalevich, Z. Hatzopoulos, P. Savvidis, and A. Kavokin, Persistent currents in half-moon polariton condensates, *ACS Photon.* **7**, 1163 (2020).
- [29] K. G. Lagoudakis, M. Wouters, M. Richard, A. Baas, I. Carusotto, R. André, L. S. Dang, and B. Deveaud-Plédran, Quantized vortices in an exciton–polariton condensate, *Nat. Phys.* **4**, 706 (2008).
- [30] D. N. Krizhanovskii, D. M. Whittaker, R. A. Bradley, K. Guda, D. Sarkar, D. Sanvitto, L. Vina, E. Cerda, P. Santos, K. Biermann, R. Hey, and M. S. Skolnick, Effect of interactions on vortices in a nonequilibrium polariton condensate, *Phys. Rev. Lett.* **104**, 126402 (2010).
- [31] D. Sanvitto, F. M. Marchetti, M. H. Szymańska, G. Tosi, M. Baudisch, F. P. Laussy, D. N. Krizhanovskii, M. S. Skolnick, L. Marrucci, A. Lemaître, J. Bloch, C. Tejedor, and L. Viña, Persistent currents and quantized vortices in a polariton superfluid, *Nat. Phys.* **6**, 527 (2010).

- [32] T. Boulier, E. Cancellieri, N. D. Sangouard, Q. Glorieux, A. V. Kavokin, D. M. Whittaker, E. Giacobino, and A. Bramati, Injection of orbital angular momentum and storage of quantized vortices in polariton superfluids, *Phys. Rev. Lett.* **116**, 116402 (2016).
- [33] B. Berger, D. Schmidt, X. Ma, S. Schumacher, C. Schneider, S. Höfling, and M. Aßmann, Formation dynamics of exciton-polariton vortices created by nonresonant annular pumping, *Phys. Rev. B* **101**, 245309 (2020).
- [34] D. Choi, M. Park, B. Y. Oh, M.-S. Kwon, S. I. Park, S. Kang, J. D. Song, D. Ko, M. Sun, I. G. Savenko, Y.-H. Cho, and H. Choi, Observation of a single quantized vortex vanishment in exciton-polariton superfluids, *Phys. Rev. B* **105**, L060502 (2022).
- [35] I. Gnusov, S. Harrison, S. Alyatkin, K. Sitnik, J. Töpfer, H. Sigurdsson, and P. Lagoudakis, Quantum vortex formation in the “rotating bucket” experiment with polariton condensates, *Sci. Adv.* **9**, eadd1299 (2023).
- [36] H. Deng, G. Weihs, C. Santori, J. Bloch, and Y. Yamamoto, Condensation of semiconductor microcavity exciton polaritons, *Science* **298**, 199 (2002).
- [37] J. Kasprzak, M. Richard, S. Kundermann, A. Baas, P. Jembrun, J. M. J. Keeling, F. M. Marchetti, M. H. Szymańska, R. André, J. L. Staehli, V. Savona, P. B. Littlewood, B. Deveaud, and L. S. Dang, Bose-Einstein condensation of exciton polaritons, *Nature* **443**, 409 (2006).
- [38] R. Balili, V. Hartwell, D. Snoke, L. Pfeiffer, and K. West, Bose-Einstein condensation of microcavity polaritons in a trap, *Science* **316**, 1007 (2007).
- [39] J. J. Baumberg, A. V. Kavokin, S. Christopoulos, A. J. D. Grundy, R. Butté, G. Christmann, D. D. Solnyshkov, G. Malpuech, G. Baldassarri Höger von Högersthal, E. Feltin, J.-F. Carlin, and N. Grandjean, Spontaneous polarization buildup in a room-temperature polariton laser, *Phys. Rev. Lett.* **101**, 136409 (2008).
- [40] T. Byrnes, N. Y. Kim, and Y. Yamamoto, Exciton-polariton condensates, *Nat. Phys.* **10**, 803 (2014).
- [41] Y. Sun, P. Wen, Y. Yoon, G. Liu, M. Steger, L. N. Pfeiffer, K. West, D. W. Snoke, and K. A. Nelson, Bose-Einstein condensation of long-lifetime polaritons in thermal equilibrium, *Phys. Rev. Lett.* **118**, 016602 (2017).
- [42] R. Su, S. Ghosh, J. Wang, S. Liu, C. Diederichs, T. C. H. Liew, and Q. Xiong, Observation of exciton polariton condensation in a perovskite lattice at room temperature, *Nat. Phys.* **16**, 301 (2020).
- [43] H. Shan, L. Lackner, B. Han, E. Sedov, C. Rupprecht, H. Knopf, F. Eilenberger, J. Beierlein, N. Kunte, M. Esmann, K. Yumigeta, K. Watanabe, T. Taniguchi, S. Klembt, S. Höfling, A. V. Kavokin, S. Tongay, C. Schneider, and C. Antón-Solanas, Spatial coherence of room-temperature monolayer WSe₂ exciton-polaritons in a trap, *Nat. Commun.* **12**, 6406 (2021).
- [44] Z. Jiang, A. Ren, Y. Yan, J. Yao, and Y. S. Zhao, Exciton-polaritons and their Bose-Einstein condensates in organic semiconductor microcavities, *Adv. Mater.* **34**, 2106095 (2022).
- [45] D. M. Whittaker, Classical treatment of parametric processes in a strong-coupling planar microcavity, *Phys. Rev. B* **63**, 193305 (2001).
- [46] I. Shelykh, L. Viña, A. Kavokin, N. Galkin, G. Malpuech, and R. André, Non-linear coupling of polariton and dark exciton states in semiconductor microcavities, *Solid State Commun.* **135**, 1 (2005).
- [47] A. Tredicucci, Y. Chen, V. Pellegrini, M. Börger, and F. Bassani, Optical bistability of semiconductor microcavities in the strong-coupling regime, *Phys. Rev. A* **54**, 3493 (1996).
- [48] A. Baas, J. P. Karr, H. Eleuch, and E. Giacobino, Optical bistability in semiconductor microcavities, *Phys. Rev. A* **69**, 023809 (2004).
- [49] A. Baas, J.-P. Karr, M. Romanelli, A. Bramati, and E. Giacobino, Optical bistability in semiconductor microcavities in the nondegenerate parametric oscillation regime: Analogy with the optical parametric oscillator, *Phys. Rev. B* **70**, 161307(R) (2004).
- [50] T. K. Paraíso, M. Wouters, Y. Léger, F. Morier-Genoud, and B. Deveaud-Plédran, Multistability of a coherent spin ensemble in a semiconductor microcavity, *Nat. Mater.* **9**, 655 (2010).
- [51] D. Schmidt, B. Berger, M. Kahlert, M. Bayer, C. Schneider, S. Höfling, E. S. Sedov, A. V. Kavokin, and M. Aßmann, Tracking dark excitons with exciton polaritons in semiconductor microcavities, *Phys. Rev. Lett.* **122**, 047403 (2019).
- [52] The dispersion of the lower branch polaritons is fitted within the coupled oscillator model as $E_{LB}(\mathbf{k}) = [E_c(\mathbf{k}) + E_x(\mathbf{k}) - \sqrt{\delta E^2(\mathbf{k}) + V_R^2}]/2$, where $E_c(\mathbf{k}) = E_{c0} + \hbar^2 k^2/2m_c^*$ is the dispersion of the microcavity photons, E_{c0} is the photon energy at the bottom of the dispersion curve, E_x is the bright exciton energy, $\delta E(\mathbf{k}) = E_c(\mathbf{k}) - E_x(\mathbf{k})$, m_c^* is the effective mass of photons in the cavity plane, and V_R is the Rabi splitting energy. The exciton and photon fractions in the polariton state are determined by the Hopfield coefficients $|X|^2 = [1 + \delta E(\mathbf{k})/\sqrt{\delta E^2(\mathbf{k}) + V_R^2}]/2$ and $|C|^2 = 1 - |X|^2$. The experimentally observed dispersion in Fig. 1(c) is best fitted for the following values of the parameters: $E_{c0} = 1.4667$ eV, $E_x = 1.471$ eV, $V_R = 6$ meV, and $m_c^* = 4.3 \times 10^{-5} m_e$, where m_e is the free-electron mass.
- [53] M. Selig, G. Berghäuser, A. Raja, P. Nagler, C. Schüller, T. F. Heinz, T. Korn, A. Chernikov, E. Malic, and A. Knorr, Excitonic linewidth and coherence lifetime in monolayer transition metal dichalcogenides, *Nat. Commun.* **7**, 13279 (2016).
- [54] M. Steger, C. Gautham, D. W. Snoke, L. Pfeiffer, and K. West, Slow reflection and two-photon generation of microcavity exciton-polaritons, *Optica* **2**, 1 (2015).
- [55] J. Schmutzler, M. Aßmann, T. Czerniuk, M. Kamp, C. Schneider, S. Höfling, and M. Bayer, Nonlinear spectroscopy of exciton-polaritons in a GaAs-based microcavity, *Phys. Rev. B* **90**, 075103 (2014).
- [56] G. Leménager, F. Pisanello, J. Bloch, A. Kavokin, A. Amo, A. Lemaître, E. Galopin, I. Sagnes, M. D. Vittorio, E. Giacobino, and A. Bramati, Two-photon injection of polaritons in semiconductor microstructures, *Opt. Lett.* **39**, 307 (2014).
- [57] M. Nithisoontorn, K. Unterrainer, S. Michaelis, N. Sawaki, E. Gornik, and H. Kano, Two-photon absorption in GaAs/AlGaAs multiple quantum wells, *Phys. Rev. Lett.* **62**, 3078 (1989).
- [58] J. S. Michaelis, K. Unterrainer, E. Gornik, and E. Bauser, Electric and magnetic dipole two-photon absorption in semiconductors, *Phys. Rev. B* **54**, 7917 (1996).
- [59] V. M. Agranovich, G. C. La Rocca, and F. Bassani, Biexcitons and dark states in semiconductor microcavities, *J. Lumin.* **76-77**, 161 (1998).

- [60] E. Blackwood, M. J. Snelling, R. T. Harley, S. R. Andrews, and C. T. B. Foxon, Exchange interaction of excitons in GaAs heterostructures, *Phys. Rev. B* **50**, 14246 (1994).
- [61] See Supplemental Material at <http://link.aps.org/supplemental/10.1103/PhysRevB.108.165411> for the nonlinear increase of the absorption observed in the sample and complementary measurements on the determination of the dark exciton energy.
- [62] M. Wouters and I. Carusotto, Parametric oscillation threshold of semiconductor microcavities in the strong coupling regime, *Phys. Rev. B* **75**, 075332 (2007).
- [63] C. Schindler and R. Zimmermann, Analysis of the exciton-exciton interaction in semiconductor quantum wells, *Phys. Rev. B* **78**, 045313 (2008).
- [64] E. Estrecho, T. Gao, N. Bobrovska, D. Comber-Todd, M. D. Fraser, M. Steger, K. West, L. N. Pfeiffer, J. Levinsen, M. M. Parish, T. C. H. Liew, M. Matuszewski, D. W. Snoke, A. G. Truscott, and E. A. Ostrovskaya, Direct measurement of polariton-polariton interaction strength in the Thomas-Fermi regime of exciton-polariton condensation, *Phys. Rev. B* **100**, 035306 (2019).
- [65] B. S. Wherrett, Scaling rules for multiphoton interband absorption in semiconductors, *J. Opt. Soc. Am. B* **1**, 67 (1984).
- [66] H. S. Pattanaik, M. Reichert, J. B. Khurgin, D. J. Hagan, and E. W. Van Stryland, Enhancement of two-photon absorption in quantum wells for extremely nondegenerate photon pairs, *IEEE J. Quantum Electron.* **52**, 1 (2016).
- [67] S. S. Gavrilov, Blowup dynamics of coherently driven polariton condensates, *Phys. Rev. B* **90**, 205303 (2014).
- [68] S. R. K. Rodriguez, A. Amo, I. Sagnes, L. Le Gratiet, E. Galopin, A. Lemaître, and J. Bloch, Interaction-induced hopping phase in driven-dissipative coupled photonic microcavities, *Nat. Commun.* **7**, 11887 (2016).
- [69] G. Muñoz-Matutano, A. Wood, M. Johnsson, X. Vidal, B. Q. Baragiola, A. Reinhard, A. Lemaître, J. Bloch, A. Amo, G. Nogues, B. Besga, M. Richard, and T. Volz, Emergence of quantum correlations from interacting fibre-cavity polaritons, *Nat. Mater.* **18**, 213 (2019).
- [70] A. Delteil, T. Fink, A. Schade, S. Höfling, C. Schneider, and A. İmamoğlu, Towards polariton blockade of confined exciton-polaritons, *Nat. Mater.* **18**, 219 (2019).
- [71] D. W. Snoke, V. Hartwell, J. Beaumariage, S. Mukherjee, Y. Yoon, D. M. Myers, M. Steger, Z. Sun, K. A. Nelson, and L. N. Pfeiffer, Reanalysis of experimental determinations of polariton-polariton interactions in microcavities, *Phys. Rev. B* **107**, 165302 (2023).